Eur. Phys. J. B **16**, 475–486 (2000)

THE EUROPEAN PHYSICAL JOURNAL B

EDP Sciences

High temperature expansion for frustrated and unfrustrated $S = \frac{1}{2}$ spin chains

A. Bühler[1,a], N. Elstner[2,b], and G.S. Uhrig[1,c]

[1] Institut für Theoretische Physik, Universität zu Köln, Zülpicher Str. 77, 50937 Köln, Germany
[2] Physikalisches Institut, Universität Bonn, Nußallee 12, 53115 Bonn, Germany

Received 24 February 2000 and Received in final form 5 April 2000

Abstract. A computer aided high temperature expansion of the magnetic susceptibility and the magnetic specific heat is presented and demonstrated for frustrated and unfrustrated spin chains. The results are analytic in nature since the calculations are performed in the integer domain. They are provided in the form of polynomials allowing quick and easy fits. Various representations of the results are discussed. Combining high temperature expansion coefficients and dispersion data yields very good agreement already in low order of the expansion which makes this approach very promising for the application to other problems, for instance in higher dimensions.

PACS. 05.10.-a Computational methods in statistical physics and nonlinear dynamics – 75.40.Cx Static properties (order parameter, static susceptibility, heat capacities, critical exponents, etc.) – 75.10.Jm Quantized spin models

1 Introduction

Spin systems are among the most investigated systems in solid state physics. They represent problems with high correlation since the spin algebra does not have the simplicity of the fermionic or the bosonic algebra. This can also be seen from the generic derivation of antiferromagnetic spin models from a half-filled Hubbard model in the limit of large interaction $U \to \infty$. Hence even the calculation of simple properties like the magnetic susceptibility χ or the magnetic specific heat C is not straightforward. Experimentally, however, susceptibility and specific heat are the first quantities used to characterise a compound. So quantitative theoretical predictions are very important to pinpoint the appropriate model.

Quantum Monte Carlo methods underwent considerable progress in the last years so that the calculation of χ and C for unfrustrated systems has become feasible to very high accuracy. The treatment of frustrated spin systems, however, is still a difficult task since in the standard Ising basis the sign problem occurs. This leads to the phenomenon that considerable cancellations and the concomitant loss of statistical accuracy occur in the quantum Monte Carlo computation, see *e.g.* reference [1]. In the case of strong frustration one still has to resort to complete diagonalisation which restrict the accessible system sizes very much, see *e.g.* reference [2]. For (quasi) one-dimensional systems like chains or ladders finite temperature density-matrix renormalisation provides a reliable means to calculate susceptibilities and specific heats, see *e.g.* references [3–6]. The caveat, however, remains that the numerical methods require a new programme run for each set of parameters. So fitting becomes a tedious task as soon as more than one parameter is involved.

The objective of the present article is to introduce a computer aided expansion in the inverse temperature for the quantities χ and C. This method is a variant of the "linked cluster" approach [7,8]. In the form implemented here it provides the results as polynomials in the relevant energy ratios. Thereby extremely fast and convenient fit procedures become possible. Frustrating terms do not pose more problems than any other additional couplings. For the sake of simplicity we will demonstrate our approach for one-dimensional systems, *i.e.* chains. The subsequent choice of an appropriate representation of the results is also very important. The inclusion of low temperature information enlarges the range of validity considerably.

In the next two sections the method is explained in detail and contrasted to the conventional linked cluster approach. In Section 4 the results are given and represented in various ways in order to obtain the best description. A particular representation based on additional dispersion data is explained in Section 5. The findings are summarised in the concluding Section 6.

[a] e-mail: ab@thp.uni-koeln.de
[b] e-mail: norbert@brahms.physik.uni-bonn.de
[c] e-mail: gu@thp.uni-koeln.de.
internet: www.thp.uni-koeln.de/~gu/

2 Methods

In the present work two methods are used to expand the physical quantities. The first one is the linked cluster method [7,8] and the second one a method which will be called moment algorithm henceforth. To be explicit, the spin-$\frac{1}{2}$ Heisenberg chain

$$H = \sum_{i=1}^{N} (J\mathbf{S}_i\mathbf{S}_{i+1} + \alpha J\mathbf{S}_i\mathbf{S}_{i+2} - hS_i^z) \tag{1}$$

with nearest and next nearest neighbour interaction is investigated with h representing the magnetic field in units of $g\mu_{\mathrm{B}}$. The ratio of nearest and next nearest neighbour exchange coupling is given by α.

The main idea of the linked cluster method is to restrict calculations to finite systems to obtain results in the thermodynamic limit. The method can be applied to systems (clusters) which are described by a sum of local Hamiltonians like the Heisenberg Hamiltonian in (1). An expansion of a quantity in powers of such a Hamiltonian results in the computation of the contributions of clusters of various sizes. To obtain the contribution of a finite cluster to the quantity of the infinite system all contributions of subclusters have to be subtracted with suitable multiplicity. Only connected ("linked") clusters provide nonvanishing contributions. The non-connected clusters cancel out due to the normalisation of the expectation value (see for instance Eq. (2)). This is the main result of the linked cluster theorem.

The numerical approach of the moment algorithm makes use of the result of the linked cluster theorem. Here as well the physical quantities are evaluated in the thermodynamic limit by means of finite systems. Let us consider the Heisenberg Hamiltonian with nearest neighbour interaction acting on a chain and let us expand a physical quantity in powers of $\beta J = J/T$, *i.e.* in powers of this Hamiltonian. The largest connected cluster at a given order n of the expansion contains $(n+1)$ sites. Hence all clusters of this size must be embedded completely in the finite system to obtain valid results in the thermodynamic limit.

For concreteness, we compute the magnetic susceptibility per site at vanishing magnetic field

$$\chi(T) = \frac{\beta}{N} \frac{\mathrm{tr}(M^2 \mathrm{e}^{-\beta H})}{\mathrm{tr}(\mathrm{e}^{-\beta H})} \,. \tag{2}$$

Denominator and numerator are computed separately by expanding the corresponding exponential functions. The resulting rational function is again expanded around $\beta = 0$ to obtain a polynomial in the inverse temperature β.

On this stage the comparison of the moment algorithm to the linked cluster approach shows one advantage and one disadvantage. The advantage is that it is not necessary to determine and to classify all contributing clusters explicitly. This task may not be underestimated in view of the lack of efficient algorithms comparing graphs. This point matters in particular for complicated lattices with different types of bonds. In this respect, the moment algorithm is simpler than the linked cluster approach. The disadvantage is that the finite systems which have to be dealt with are fairly large, in particular for elevated orders in β and higher dimensions. In this respect, the linked cluster approach is better suited for higher dimensional problems.

The disadvantage mentioned is less troublesome if an efficient way to compute traces of powers of the Hamiltonian is available. To this end we present an algorithm which computes such traces in a very fast way. "Fast" means that the necessary effort increases not exponentially with system size N but only in powers of N. The algorithm reduces the trace to an ordinary expectation value in a higher-dimensional Hilbert space. To this purpose the Hilbert space of the real system is doubled by introducing to each real site $|i_{\mathrm{r}}\rangle$ a "doubled" site $|i_{\mathrm{d}}\rangle$. Any operator A defined on the real Hilbert space acts on the tensor product of real and doubled Hilbert space in the canonical way. That is A becomes $A \otimes 1$ acting as the identity on the doubled Hilbert space.

Furthermore, we consider a state which is the (unnormalised) product of singlets (or triplets with $S^z = 0$) between the real and the doubled sites

$$|S\rangle = \prod_{i=1}^{N} (|\uparrow_{\mathrm{r}}\downarrow_{\mathrm{d}}\rangle - |\downarrow_{\mathrm{r}}\uparrow_{\mathrm{d}}\rangle)\big|_i. \tag{3}$$

The key observation is that the trace in the original, real Hilbert space is identical to the expectation value of $|S\rangle$ in the extended Hilbert space

$$\mathrm{tr}(A)|_{\mathrm{real}} = \langle S|A \otimes 1|S\rangle \;|_{\mathrm{double}}. \tag{4}$$

To see the identity (4) one considers first a single site. Explicit calculation shows

$$\begin{aligned} \mathrm{tr}(A)|_{\mathrm{real}} &= \langle\uparrow|A|\uparrow\rangle + \langle\downarrow|A|\downarrow\rangle && \text{(5a)} \\ &= \langle\uparrow_{\mathrm{r}}\downarrow_{\mathrm{d}}|A|\uparrow_{\mathrm{r}}\downarrow_{\mathrm{d}}\rangle|_{\mathrm{d}} + \langle\downarrow_{\mathrm{r}}\uparrow_{\mathrm{d}}|A|\downarrow_{\mathrm{r}}\uparrow_{\mathrm{d}}\rangle|_{\mathrm{d}} && \text{(5b)} \\ &= \langle S|A|S\rangle|_{\mathrm{d}} && \text{(5c)} \end{aligned}$$

where we used the subscripts r and d for "real" and "doubled" (extended) Hilbert space, respectively. The validity of (4) follows from (5a) directly for all operators A which are products of local spin operators since the Hilbert space of many spins is just the tensor product of the Hilbert spaces of the individual spins

$$\begin{aligned} &\mathrm{tr}\prod_i A_i|_{\mathrm{r}} = \prod_i \mathrm{tr} A_i|_{\mathrm{r}} && \text{(6a)} \\ &= \prod_i \langle(\langle\uparrow_{\mathrm{r}}\downarrow_{\mathrm{d}}| - \langle\downarrow_{\mathrm{r}}\uparrow_{\mathrm{d}}|)A_i(|\uparrow_{\mathrm{r}}\downarrow_{\mathrm{d}}\rangle - |\downarrow_{\mathrm{r}}\uparrow_{\mathrm{d}}\rangle)\rangle|_i && \text{(6b)} \\ &= \langle S|\prod_i A_i|S\rangle|_{\mathrm{d}}. && \text{(6c)} \end{aligned}$$

From the linearity of the expectation value and the trace follows then that (4) holds also for all operators A since they can be decomposed into sums of products of local spin operators.

On the left hand side of (4) for $A = H^2$ for instance one has to compute in the Ising basis (spins up or down) 2^N contributions for L^2 terms (N number of sites, L number of bonds), *i.e.* one has to sum about $L^2 2^N$ terms. On the right hand side of (4), however, one starts with a single state which will be excited in L ways by the application of $H \otimes 1$ and requires to be de-excited in the same way so that only L terms contribute in the end. Thus one saves an exponential factor. An obvious by-product are the relations

$$\begin{aligned} \langle S|H^{2n}|S\rangle &= \langle S|H^n H^n|S\rangle \\ &= |H^n|S\rangle|^2 \qquad (7a) \\ \langle S|H^{2n+1}|S\rangle &= \langle S|H^n H^{n+1}|S\rangle \qquad (7b) \end{aligned}$$

which imply that for a given order m in β one needs to calculate only about $m/2$ applications of H to the singlet product state $|S\rangle$. This statement remains true for the numerator of susceptibilities as in (2) if the observable (here: $M = \sum_{i=1}^{N} S_i^z$) commutes with H. This is the case for the uniform magnetisation M. Replacing $|S\rangle$ by $M|S\rangle$ thus makes the relations (7) also applicable to the numerator of (2).

We implemented the actual calculations on computer. For not too high orders this can still be done with computer algebra programmes. But to obtain the highest orders it is necessary to write task-specific programmes. This was done by using the language C^{++}. Yet the dependencies on all coupling constants are included on the symbolic level, *i.e.* in polynomials of the coupling constants. So, once obtained, the results are available to everybody and they can be fitted to any experimental curve very quickly and easily. The results for the moment algorithm (frustrated (order 10) and unfrustrated spin chain (order 16)) and for the linked cluster algorithm (unfrustrated spin chain only, but order 24) are presented in the appendix.

Before concluding this section we like to note that the trick to pass from a trace to an expectation value in a higher dimensional Hilbert space is not restricted to spin-$\frac{1}{2}$ systems. By introducing for instance the generalised product state of singlets $|S\rangle_g$

$$|S\rangle_g = \prod_j \sum_{i=0}^{2S} \frac{(-1)^i}{\sqrt{2S+1}} |(S-i)_\mathrm{r}, (i-S)_\mathrm{d}\rangle\Big|_j \qquad (8)$$

the method can be applied to arbitrary spin. In (8) $|j_\mathrm{r}, l_\mathrm{d}\rangle$ stands for the state where the real spin has $S^z = j$ and the doubled spin $S^z = l$. For a derivation one simply has to redo the calculation (5).

Henceforth the angular brackets will denote the expectation value with regard to $|S\rangle$ or the original trace, respectively, since their identity is established and so no further distinction necessary.

The calculations in the present work were done to the highest order possible on the available work stations. For the unfrustrated chain the physical quantities were expanded to order N on a finite system of size N sites. Therefore clusters in the Nth order are overcounted or missed. But it is possible to correct these effects in highest order by an analytical argument which is presented in the subsequent section.

3 Finite size corrections

The wrap-around effects of the numerator and denominator of equation (2) are investigated separately for a chain of length N with periodic boundary conditions.

The denominator has the following kind of contributions in the Nth order

$$\langle H^N \rangle = \langle \prod_{i=1}^{N} (\mathbf{S}_i \mathbf{S}_{i+1}) \rangle + \dots \qquad (9)$$

which are not realised in the thermodynamic system. Fixing the component of one of the spin vectors involved to for instance S^x one sees that a non-vanishing contribution occurs only if all spin components are S^x. The overall value of the right hand side in (9) is 4^{-N}. Since all permutations of the scalar products will occur as well if the left hand side of (9) is expanded and since all these permutations yield the same contribution the factor $N!$ has to be added. Since the choice of the spin component was arbitrary an additional factor 3 concludes the argument. Thus one has to subtract $3N!4^{-N}$ to yield the thermodynamic result in the denominator.

The corrections of the numerator of equation (2) are more complicated. They consist of three contributions. The first is similar to the one in the denominator

$$\langle (S_1^z)^2 H^N \rangle = \langle (S_1^z)^2 \prod_{i=1}^{N} (\mathbf{S}_i \mathbf{S}_{i+1} \rangle + \dots \qquad (10)$$

and overcounts the numerator by $3N!4^{-N-1}$. On the other hand, the thermodynamic contribution is neglected in this order of expansion

$$\langle S_1^z S_{N+1}^z (\mathbf{S}_1 \mathbf{S}_2)(\mathbf{S}_2 \mathbf{S}_3) \dots (\mathbf{S}_N \mathbf{S}_{N+1}) \rangle \qquad (11)$$

which represents the second correction. It takes the value $2N!4^{-N-1}$. The factor $N!4^{-N-1}$ arises for the same reasons as before. There is no factor 3 since the spin component is already fixed by the choice of the magnetisation direction. The geometric factor 2 arises instead because the sites 2 to $N+1$ can be found to the right or to the left of the starting site 1.

The third and last correction consists of clusters with triple occurrence of two sites. It is based on the identity for $S = 1/2$

$$S^x S^y S^z = i/8 \qquad (12)$$

which holds also for all cyclic permutations of the spin components. For anticyclic permutations the left hand side of (12) acquires a minus sign.

A wrap-around with sites occurring three times is possible as soon as the magnetisation operators are taken to

be at different sites: $S_1^z S_j^z$ with $j \neq 1$. Then each of the sites 1 and j appears three times

$$\langle S_1^z S_j^z \prod_{i=1}^{N} (\mathbf{S}_i \mathbf{S}_{i+1} \rangle. \tag{13}$$

Note that all permutations of the sequence of the scalar products appear. Hence in most cases the contributions cancel each other since cyclic and anticyclic permutations of the spin components at site 1 or site j occur independently and with equal amplitude. Only if the site j is adjacent to 1, *i.e.* $j = 2$ or $j = N$ (periodic boundary conditions), the cyclic and anticyclic permutations at site 1 and j are correlated and a finite total effect remains. The relevant factors are (for $j = 2$)

$$\langle S_1^z S_2^z (\mathbf{S}_N \mathbf{S}_1)(\mathbf{S}_1 \mathbf{S}_2)(\mathbf{S}_2 \mathbf{S}_3) \dots \rangle. \tag{14}$$

Among the $3! = 6$ ways to arrange the three scalar products in (14) the two where $(\mathbf{S}_1 \mathbf{S}_2)$ is in the middle yield $1/8^2(S_N^x S_3^x + S_N^y S_3^y)$ while the other four yield $-1/8^2(S_N^x S_3^x + S_N^y S_3^y)$ so that $-2/8^2(S_N^x S_3^x + S_N^y S_3^y)$ remains. Accounting for the multiplicity due to the arrangement of the other scalar products yields the combinatorial factor $N!/3!$. A factor 2 comes from the possibility to choose $j = 2$ or $j = N$. The overall third correction finally reads $-8 \times 4^{-(N+1)} N!/3!$

In summary, the total corrections to the results computed in the Nth order for a finite system of N sites with periodic boundary conditions for the numerator Nu and for the denominator De are

$$\mathrm{Nu}_{\mathrm{corrected}} = \mathrm{Nu}_{\mathrm{computed}} + N! \, \frac{1}{3} \left(\frac{1}{4} \right)^{N+1} \tag{15a}$$

$$\mathrm{De}_{\mathrm{corrected}} = \mathrm{De}_{\mathrm{computed}} - N! \, 3 \left(\frac{1}{4} \right)^{N}. \tag{15b}$$

After these considerations it is also straightforward to correct the wrap-around effects for the Heisenberg chain with next-nearest neighbour interaction. In the Nth order on a finite system of $2N$ sites these effects occur only in the Nth order in α and in β. In this order the system corresponds to a system of two independent chains with nearest neighbour interactions only, so that the corrections (15) apply to terms of Nth order in α. This concludes the discussion of the finite size corrections.

4 Results and representations

In the Appendix the series coefficients are presented for the magnetic susceptibility χ and for the magnetic specific heat C per site. The specific heat is derived from the denominator of equation (2) which is the partition function of the system by

$$C(T) = \frac{1}{N} \frac{\partial}{\partial T} \frac{\langle H \mathrm{e}^{-\beta H} \rangle}{\langle \mathrm{e}^{-\beta H} \rangle} \tag{16a}$$

$$= \frac{1}{N} \frac{\partial}{\partial T} \left(\frac{-\frac{\partial}{\partial \beta} \langle \mathrm{e}^{-\beta H} \rangle}{\langle \mathrm{e}^{-\beta H} \rangle} \right). \tag{16b}$$

It is worth mentioning that due to the derivation in (16b) one order in β is lost. It is re-gained, however, by the subsequent derivation with respect to T.

In particular, results for the unfrustrated chain are listed in Appendix A.3. These are obtained by the linked cluster method and comprise orders as high as 24. Such high orders are obtained by an exact extrapolation of smaller clusters as explained below. They are in agreement with expansion results previously obtained [9, 10]. In Appendix A.3.1 the magnetic susceptibility coefficients are given, in Appendix A.3.2 the specific heat coefficients are given.

For the loop-free chain the calculation of high temperature series for spin models simplifies decisively compared to higher dimensions due to the simple structure of the contributing cluster. A finite open chain with n bonds will contribute to the specific heat only in order β^{2n}. This is so because otherwise there will always be one site occurring an odd number of times in the spin products leading eventually to a vanishing trace.

The susceptibility series shows a systematic pattern which can be exploited to obtain longer series. For the $S = 1/2$ Heisenberg chain, the nonvanishing contribution of order β^n of a finite open cluster with n bonds and $n+1$ sites will be due to one spin product of the Hamiltonian acting on each bond and two magnetisation operators S^z at the ends of the chain. Its contribution is of the form $a_0 n! \, 4^{-n-1} \beta^n$, where a_0 is independent of the cluster size (as before we consider the terms without the $1/n!$ factors from the exponential series).

Similarly, the contribution in order β^{n+1} will be of the form $(b_0 + n b_1) n! \, 4^{-n-2} \beta^{n+1}$. Again b_0 and b_1 do not depend on the length of the finite cluster. The term proportional to n is due to the n possibilities to attach one more term of the Hamiltonian to any of the n bonds.

In the same way, the general form of the higher order contributions can be determined with more and more coefficients. With sufficiently large clusters the coefficients a_0, (b_0, b_1), (c_0, c_1, c_2), ... can be obtained by solving a system of linear equations. Using clusters with up to 18 bonds allowed to extend the susceptibility series to order 24.

The moment algorithm allowed us to compute results for the unfrustrated chain up to order 16 for the susceptibility (A.1.1) and for the specific heat (A.2.2). Note that this is only two orders less than the maximum cluster which is actually computed in the linked cluster approach. The results are in complete agreement with the linked cluster results. The only difference is in the internal representation where doubles are used in the linked cluster programme and true fractions in the moment algorithm. The susceptibility as well as the specific heat of the frustrated chain is expanded up to order 10 (A.2.1 and A.2.2).

Having obtained the series for the various expansions we pass now to the discussion of suitable representations. The choice of an appropriate representation allows to gain the maximum of information from the bare series coefficients. We follow two main routes. One is the use of Padé approximants and continued fractions, respectively; the other is to incorporate additional information at low

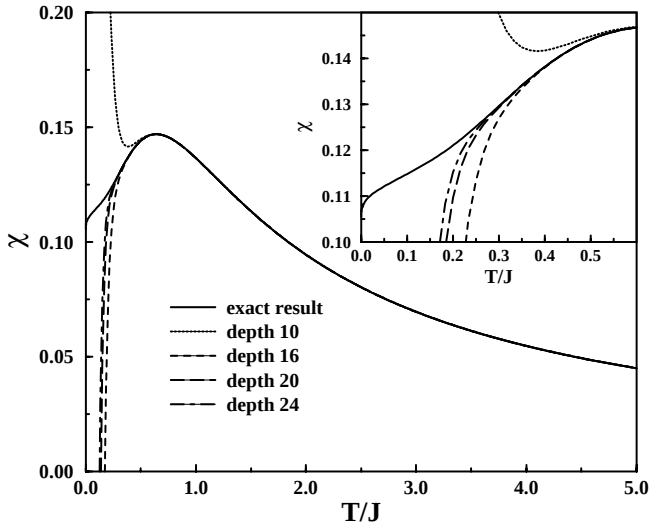

Fig. 1. Comparison of various depths of continued fraction representations of the susceptibility χ for the unfrustrated chain.

temperatures to improve the representations in the low temperature regime.

Exact results from Bethe ansatz calculations for the unfrustrated chain [11, 12] and numerical results from density-matrix renormalisation group (DMRG) calculations for the frustrated chain [13] are used as benchmarks.

4.1 Unfrustrated chain

Since the convergence of the plain series in β can be hindered by any pole the use of a Padé approximant describing the quantity under study by a rational function is more stable than the plain series.

The polynomial in β of the physical quantity under consideration is represented as a continued fraction, say with depth $2N$,

$$\chi[2N](\beta) = \cfrac{\beta}{c_1 + \cfrac{\beta}{c_2 + \cfrac{\ddots}{\cdots + \cfrac{\beta}{c_{2N}}}}} \tag{17}$$

which is equivalent to the $[N, N]$ Padé approximant. An odd depth of $2N+1$ is equivalent to the $[N+1, N]$ Padé approximant. Increasing the degree of either the numerator or the denominator polynomial at the expense of the other does not improve the results. The advantage of the continued fraction representation is that the coefficients c_i remain constant on increasing depth. For instance c_1 is equal to 4 and c_2 is equal to $1/2$ due to the Curie and due to the Curie-Weiss law, respectively.

In Figure 1 various depths of continued fraction representations of the unfrustrated susceptibility are shown. The comparison with the exact result shows that the agreement improves on increasing depth as expected. But the improvement of the representations is relatively small for higher depths. Excellent agreement can be achieved down to $T \approx J/4$ if coefficients up to order 24 are used.

In order to extend the region of satisfying agreement to lower temperatures information about the low temperature regime can be incorporated. To this end, the continued fraction depth is incremented by adding a new constant. This constant is not determined from the high temperature expansion. But it is determined such that the desired additional property is fulfilled.

To be precise, we include the value of the susceptibility at zero temperature. For the unfrustrated chain it can be expressed as [11, 14]

$$\chi(0) = \frac{1}{2\pi}\frac{1}{v_\mathrm{S}} \tag{18}$$

with the spin wave velocity $v_\mathrm{S} = \frac{\pi}{2}$ [15]. Equation (18) implies that the central charge c is one. Assuming that the central charge does not vary on switching on the frustration we will use (18) there, too. For the change of the spin wave velocity is accounted by [16] by

$$v_\mathrm{S} = \frac{\pi}{2}(1 - 1.12\alpha) \quad \text{for} \quad 0 \le \alpha < \alpha_\mathrm{c}. \tag{19}$$

In the gapped regime for $\alpha \ge \alpha_\mathrm{c} \approx 0.241167$ [17] the susceptibility vanishes exponentially at $T = 0$.

The relevant gap, however, is not the spectroscopic gap Δ_{01} between the $S = 0$ ground state and $S = 1$ excited states but half of this value $\Delta_{01}/2$. This is so since the elementary excitations of strongly frustrated spin chains are asymptotically free massive $S = 1/2$ spinons, see for instance references [18–20].

The low temperature behaviour of the specific heat [11] is given by

$$C(T \approx 0) = \frac{\pi}{3}\frac{1}{v_\mathrm{S}}T \tag{20}$$

with the same spin wave velocities v_S as in the previous equations for $\alpha < \alpha_\mathrm{c}$. In the gapped regime for supercritical frustration, an exponential vanishing for low temperatures is to be expected. From (20) follows directly

$$\frac{\mathrm{d}}{\mathrm{d}T}C(T = 0) = \frac{\pi}{3}\frac{1}{v_\mathrm{S}} \tag{21}$$

which can also be incorporated in the representations. A third piece information is obtained by

$$s(\infty) - s(0) = \int_0^\infty \frac{C(T)}{T}\mathrm{d}T = \ln 2. \tag{22}$$

This piece of information, however, is more difficult to build-in since it involves an integration over the continued fraction. Moreover, it turns out that its effect is not sizable. Thus it is not considered any further.

Figure 2 shows the various representations for the susceptibility χ of the unfrustrated chain. The approximate results agree very well with the exact ones down to

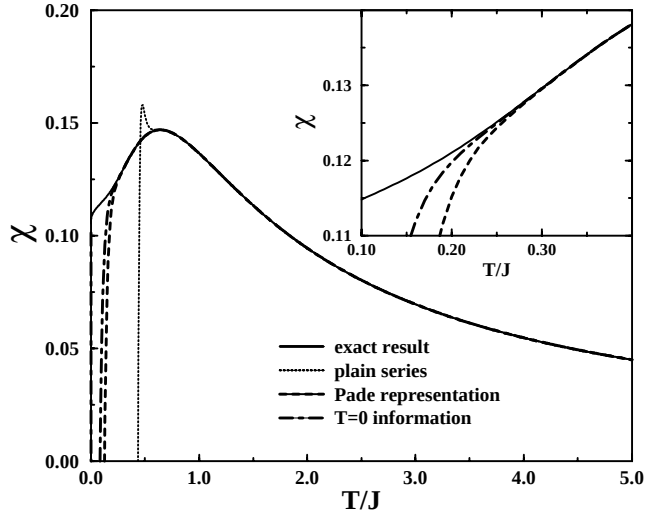

Fig. 2. Various representations of the susceptibility χ for the unfrustrated chain. The plain series is expanded up to order 24. The inset shows a zoom of the [12,11]-Padé approximant and of the [12,12]-Padé approximant with $T = 0$ information, see equation (18).

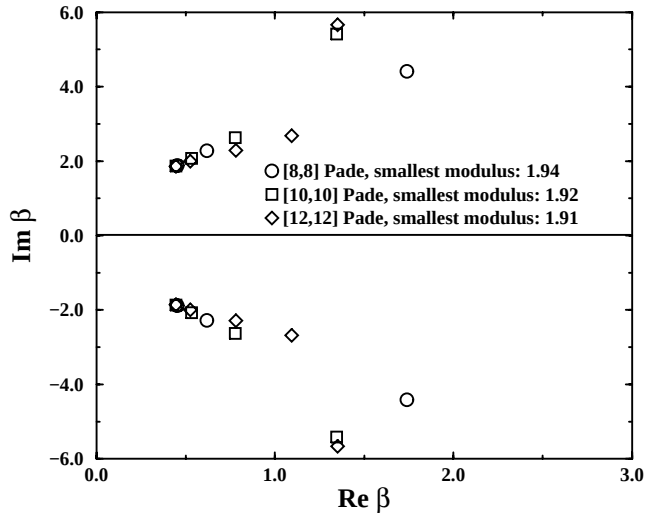

Fig. 3. Singularities of various Padé representations in β for χ and the smallest moduli of their β values. Singularities in the left half-plane are not shown.

$T/J \approx 0.2$ for the Padé approximant with $T = 0$ information. Without the aid of the exact result one is also able to determine the quality of the representation by comparison of results in highest order with those in lower orders.

It is instructive to look at the poles of the Padé representations closest to the origin. Their modulus is an estimate for the radius of convergence of the plain series. From the values given in Figure 3 one can deduce that this value is fairly constant at about $\beta_{\max} \approx 1.9$. This implies that the plain series will always diverge below about $T \approx 0.53$ irrespectively of the order of the series, *cf.* Figures 1, 2. This is a good illustration of the utility of Padé representations. They are not blocked by the occurrence of poles. So they are able to represent more complicated functional dependencies.

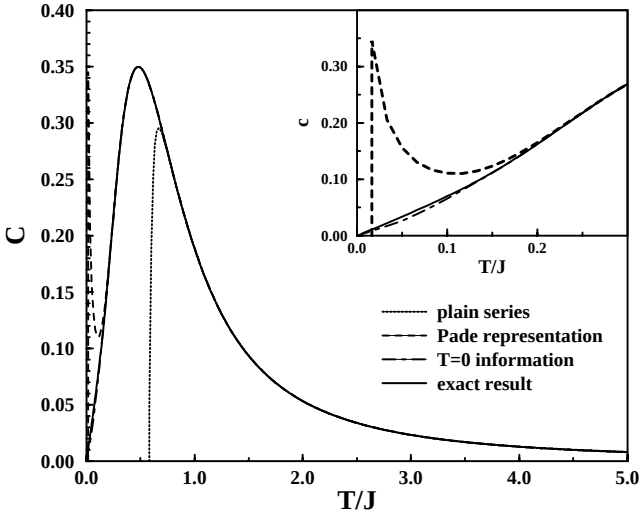

Fig. 4. Various representations of the specific heat C for the unfrustrated chain. The plain series is expanded up to order 24. The inset shows a zoom of the [11,11]-Padé approximant and of the [12,12]-Padé approximant with $T = 0$ information, see equations (20) and (21).

The low temperature behaviour of the specific heat is less complex than the one of the susceptibility. Figure 4 shows a better agreement with the exact result, especially in the low temperature regime. Here the plain series is expanded up to order 24 in β. With the two pieces of low temperature information (20, 21) the representation agrees very well with the exact result down to $T/J \approx 0.1$.

At this stage a consideration of the range of validity that one could expect is in order. In fact, we argue that one should have expected an even better description based on $1/T$ results.

Calculating up to order n means that the physics on a length scale n (lattice constant set to unity) is taken into account since this is the size of the maximum cluster treated properly. So one is led to the estimate

$$n \approx \frac{v_{\mathrm{S}}}{2\pi T_{\min}} \tag{23}$$

where the energy scale $2\pi T_{\min}$ results from the discretisation of the Matsubara frequencies which serves here as infrared cutoff. From (23) follows for the unfrustrated chain $T_{\min} \approx 1/(4n)$ for the temperature down to which the large T information should be capable to describe the physics properly. It is obvious that the validity stops actually at much higher temperatures. For this reason we presume that the representation by a Padé approximant is not yet the optimum.

4.2 Frustrated chain

Motivated by the inorganic spin-Peierls system $CuGeO_3$ [21, 22] the results for the frustrated chain are presented with a fixed α-value of 0.35 [23–25]. This value is chosen since it allows a good description of the susceptibility data. At low temperatures there is evidence that the frustration is lower [26].

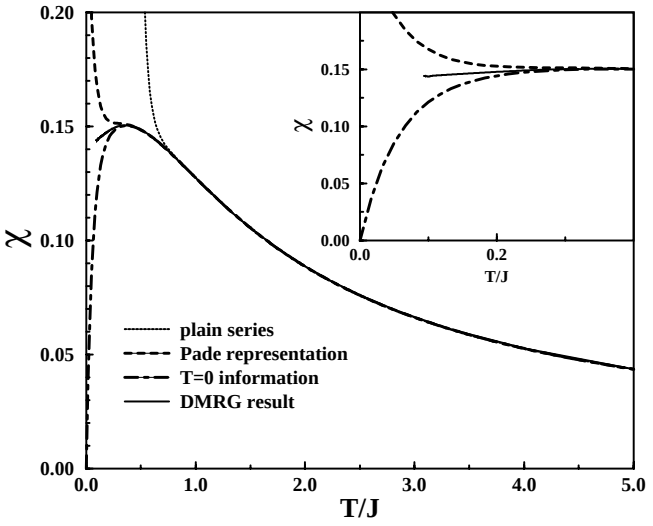

Fig. 5. Various representations of the susceptibility χ for the frustrated chain with $\alpha = 0.35$. The plain series is expanded up to order 10. The inset shows a zoom of the [5,4]-Padé approximant and of the [5,5]-Padé approximant with $T=0$ information for the gapped regime.

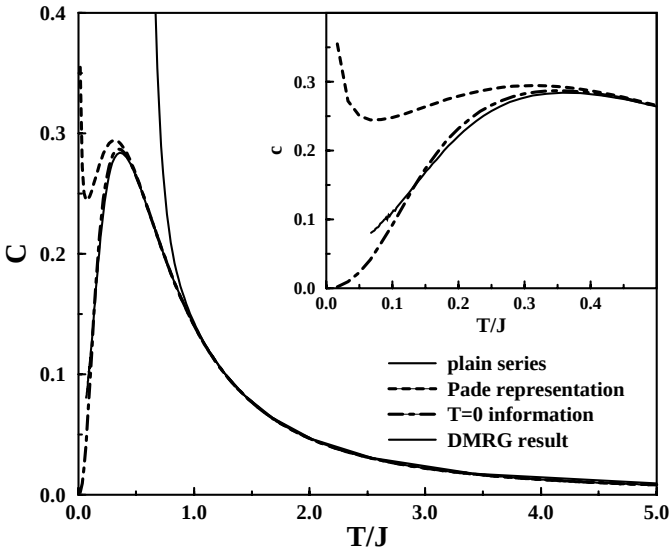

Fig. 6. Various representations of the specific heat C for a frustrated chain with $\alpha = 0.35$. The plain series is expanded up to order 10. The inset shows a zoom of the [4,4]-Padé approximant and of the [5,5]-Padé approximant with $T=0$ information, see equations (20) and (21).

Comparisons to benchmark calculations were also performed at the critical frustration α_c. Compared to the higher orders reached in the unfrustrated case, the results for the frustrated chain should agree well only for higher values of T/J. We will see, however, that this is not the case.

Figure 5 shows the susceptibility compared to DMRG calculations. The best representation with $T = 0$ information is in very good agreement down to $T/J \approx 0.25$.

Since the frustration is supercritical $0.35 > \alpha_c$ the $T = 0$ information consists in fixing $\chi(T = 0) = 0$ due to the exponential vanishing. The region of satisfying agreement coincides very well with the one of the representation of the specific heat C with $T = 0$ information in Figure 6. For the specific heat in the supercritical regime the derivative $\mathrm{d}C/\mathrm{d}T$ is set to zero, too.

Obviously, frustration is favourable for the range of applicability of the $1/T$ expansion. Without frustration we had to include much higher orders to achieve similar agreement down to $T/J \approx 0.25$. Figures 5 and 6 depict data for a specific value of frustration. But the raw data as given in Appendix A.2 allow the calculation of susceptibilities and specific heats for any value of frustration.

Three possible sources for the improvement of the $1/T$ description by frustration are conceivable. One is the appearance of a gap due to frustration. But for $\alpha = \alpha_c$ we found qualitatively the same behaviour so that this explanation can be excluded. A second idea concerns the dominance of logarithmic corrections. Since our ansätze are not fit to represent these corrections the agreement must deteriorate once logarithmic corrections become important on lowering the temperature. If this mechanism were the dominant one should expect a significantly improved agreement at the critical frustration. The actual comparison (not shown), however, does not display a significantly improved agreement. So the logarithmic corrections seem to be not the main problem of a correct representation [27].

The third possible explanation is a reduction of the spin wave velocity or, put differently, of the whole dispersion. Analytically, it is known in leading order of an expansion around the dimer limit that frustration lowers the mobility of the excitation [28]. Numerical results show the same, (see Eq. (19)). Indeed, the positions of the maxima and the lower bound of the range of validity scale roughly like the spin wave velocity as given by equation (19). Hence, our results indicate that the estimate (23) is valid to the extent that it establishes a proportionality $T_{\min} \propto v_S/n$.

Summarising this section we state that the Padé representations with low temperature information incorporated show very good agreement down to rather low values of T/J. In particular the maxima of the physical quantities susceptibility and specific heat are sufficiently well-described. With the full dependence of the model parameter one has a powerful tool to fit the parameters to experimental data in a very fast and convenient way.

5 Representation with dispersion data

In this section a different kind of representation is illustrated. It is also based on the idea to incorporate low temperature information in a high temperature expansion. As in the previous section, the approach is motivated by approximations for the susceptibility of a dimerised and frustrated $S = \frac{1}{2}$ chain in references [29, 30]. There the authors approximate the magnetic susceptibility by using

an exclusion statistics appropriate for excited triplets in the dimer model. To first approximation these excitations are often treated as free bosons. Yet it is obvious that they are hard-core bosons since there cannot be more than one on each dimer. This basic fact was included in reference [29]. In reference [30] the interaction beyond the hard-core exclusion was incorporated on a mean-field level.

Defining the partition function

$$z(\beta) = \frac{1}{2\pi} \int_{-\pi}^{\pi} \mathrm{d}k \; \mathrm{e}^{-\beta\omega(k)}, \tag{24}$$

for a single excitation one obtains the hard-core

$$\chi_0 = \beta \frac{z(\beta)}{1 + 3z(\beta)} \tag{25}$$

for the hard-core exclusion statistics. On the mean-field level one obtains

$$\chi = \frac{\chi_0}{1 + J_{\mathrm{eff}}\chi_0} \tag{26}$$

where J_{eff} can be determined either in the limit of strong dimerisation or in such a way that the Curie-Weiss constant is correct. Both methods do not differ much [30]. The approach (26) is very successful in describing triplets with small dispersion [31] as in $SrCu_2(BO_3)_2$ [32].

Formulae (25, 26) suggest to represent $T\chi$ essentially as function of $z(\beta)$. In the lowest order the representation should reproduce equation (25). Furthermore, it should allow to incorporate the information of the high temperature expansion in a natural way and the ansatz should be as simple as possible. Our choice is

$$T\chi = \cfrac{c_0 z(\beta)}{1 + \cfrac{c_1 v(\beta)}{1 + \cfrac{c_2 v(\beta)}{1 + c_3 v(\beta) \cdots}}} \tag{27}$$

with

$$v(\beta) = 1 - z(\beta). \tag{28}$$

The variable $v(\beta)$ is chosen such that $v(\beta) \propto \beta$ for $\beta \to 0$ so that the coefficients in (27) can be determined straightforwardly from the high temperature expansion. Of course, the choice (27) is just one of many possible choices so that a certain degree of arbitrariness remains. We tried also other choices, for instance an ansatz extending (26) where χ_0 is taken as variable instead of v. Our observation is that the particular choice does not matter much so that we present here the easiest ansatz we could think of.

The low temperature information incorporated in (27) is in the dispersion relation $\omega(k)$. In order to demonstrate the approach we apply it to the unfrustrated chain where we can rely on exact results for the dispersion [15]

$$\omega(k) = \frac{\pi}{2} \sin(k). \tag{29}$$

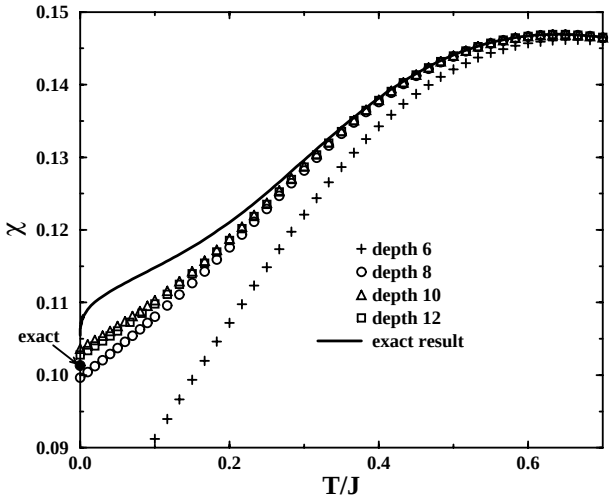

Fig. 7. Various orders of continued fraction representations of equation (27) for the magnetic susceptibility of a Heisenberg chain in comparison to the exact result obtained by Bethe ansatz. The arrow indicates the exact result at $T = 0$.

We are aware that the unfrustrated case is not particularly suited for the approach (27) as motivated above. The elementary excitations are $S = 1/2$ spinons [33], not magnons. In this respect, we are choosing a difficult test case for which we will show that the approach works very well. On the other hand, it is known that the main weight of the dynamic structure factor [14,34] is located close to the lower boundary given by (29) so that the use of (29) as "magnon dispersion" is justifiable.

Evaluation of the integral (24) yields

$$z(\beta) = I_0\left(\frac{1}{2}\beta\pi\right) - L_0\left(\frac{1}{2}\beta\pi\right) \tag{30}$$

with the modified Bessel function of the first kind I_ν and the modified Struve function L_ν as defined in reference [35].

By construction, the ansatz (27) is able to fulfill the high temperature limit $\beta \to 0$ where $T\chi \to 1/4$. It does so if c_0 is set to $1/4$. It is a very favourable feature that the opposite limit of vanishing temperature $\beta \to \infty$ where $T\chi \to T/\pi^2$ [36,37] can also be reproduced. Using

$$z(\beta) = 2/\pi \int_0^{\pi/2} \mathrm{e}^{-\beta\pi/2\sin(k)}\mathrm{d}k \tag{31a}$$

$$\underset{\beta\to\infty}{=} 2/\pi \int_0^{\infty} \mathrm{e}^{-\beta\pi/2k}\mathrm{d}k = 4/(\beta\pi^2) \tag{31b}$$

one easily sees that the correct $T \to 0$ limit is obtained if

$$1 = 4c_0/(1 + c_1/(1 + c_2/(1 + c_3/\cdots))) \tag{32}$$

holds.

Figure 7 shows various continued fraction representations of the magnetic susceptibility of a Heisenberg chain. Already low orders of the representation show good agreement with the exact result down to low T/J. Even the sixth order representation describes position and height of

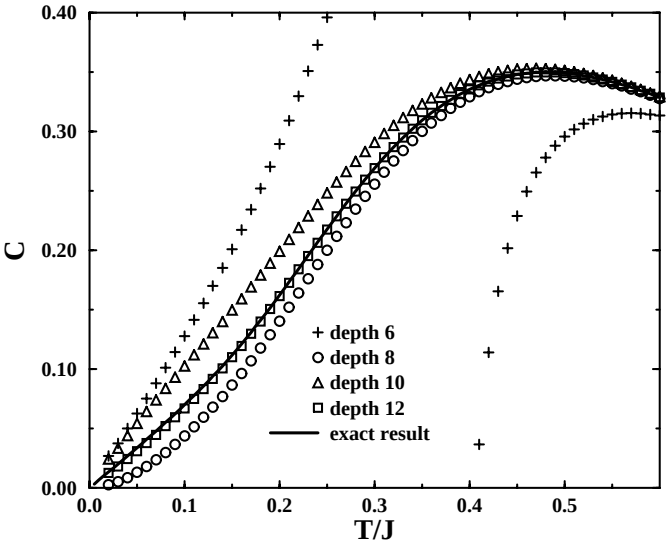

Fig. 8. Various orders of continued fraction representations of equation (33) for the specific heat of a Heisenberg chain in comparison to the exact result obtained by Bethe ansatz.

the maximum fairly well. For order 8 and above, the maximum is perfectly described. Even the value of the zero temperature susceptibility is very close to its exact value which could not be expected since the validity of (32) is not built-in.

The 12th order representation fits very well down to $T/J \approx 0.3$, which is almost the result of the $[12, 12]$-Padé approximant in Figure 2 obtained from a much costlier series up to order 24. Orders above 12 are difficult to implement with the dispersion information since the determination of the constants c_i becomes very tedious. Parallely, the improvement obtained becomes smaller and smaller.

Looking at Figure 7 closely it can be concluded that only the logarithmic terms in the susceptibility [12, 38] spoil the agreement at low temperatures $T/J < 0.3$. If these terms are explicitly incorporated the agreement in the whole temperature range can be conveniently described [6].

It is, however, not our aim to provide a fit to a result which is known analytical. For this reason we do not follow the route to incorporate the logarithmic terms into the ansatz (27). By the results depicted in Figure 7 we have demonstrated that the inclusion of $T = 0$ information in an ansatz of high temperature expansion improves the range of validity considerably. In particular, already a small number of high temperature coefficients allows a satisfyingly accurate description of the overall form of the physical quantity under study. To corroborate this conclusion we present in Figure 8 the analogous result for the specific heat. It is based on the ansatz

$$C = \frac{3}{2}\beta^2 \frac{d_0\left(z'' - 3(z')^2/(1+3z)\right)}{1 + \dfrac{d_1 v(\beta)}{1 + \dfrac{d_2 v(\beta)}{1 + d_3 v(\beta) \cdots}}} \qquad (33)$$

where z' and z'' stand for the first and the second derivative of z with respect to β, respectively. The ansatz (33) is motivated by the result

$$C = \frac{3}{2}\beta^2 \frac{\left(z'' - 3(z')^2/(1+3z)\right)}{1+3z} \qquad (34)$$

derived from the free energy including exclusion statistics [29]. As for the susceptibility the agreement between approximate ansatz and exact results is good even for low depths of the continued fraction (33). Note, however, the spurious pole at about $T = 0.3J$ occurring in the representation of depth 6. This phenomenon cannot be excluded in Padé representations so that one should always consider various depths in order to judge which features are meaningful. The 12th order result agrees excellently with the exact result which shows the efficiency of the ansatz (33).

Against the ansätze (27, 33) one may object that the dispersion $\omega(k)$ will not be available in general. Of course, exact results for the dispersion are as rare as exact results for susceptibilities or specific heats. But there are a number of good approximate methods which provide $\omega(k)$ at zero temperature, for instance perturbative expansions [39]. Their results can be taken to refine and to supplement the high temperature expansions. Or it can be reasonable to use the experimentally determined results for $\omega(k)$ in order to understand the thermodynamic quantities.

The fact that already low orders of a high temperature expansion can be sufficient to provide good estimates for $\chi(T)$ and $C(T)$ is especially important for higher dimensional models in $d = 2$ or $d = 3$. In these cases higher orders cannot be obtained due to the quickly rising number of sites or number of clusters to be considered.

6 Summary

The main objective of the present paper is to illustrate a general way to obtain very fast and convenient analytical formulae for standard thermodynamical quantities such as the magnetic susceptibility and the specific heat. So the results should be viewed mainly as effective tools for quick data analysis. The route to such formulae comprises two steps. The first one is a high temperature expansion in β performed symbolically on computers providing the coefficients in analytic form. The second one is the use of an optimised representation of the results. In this second step the inclusion of additional information at zero temperature available from other sources is particularly useful. It is not our objective to compute by the methods presented unknown low temperature physics.

For the sake of illustration we considered in the present article frustrated Heisenberg chains, *i.e.* chains of $S = 1/2$ spins with nearest and next-nearest neighbour couplings J and αJ, respectively. For these chains we provided the high temperature coefficients for the magnetic susceptibility and the specific heat up to order 10 in the frustrated case and up to order 24 in the unfrustrated case.

For topologically simple lattices the linked cluster approach is the most efficient since it avoids to compute powers of the Hamiltonian on unnecessarily large systems. The actual expansion is done for subsystems, the so-called clusters. The price to pay is the necessary sophisticated bookkeeping of the clusters.

In order to be able to treat straightforwardly also more complicated lattices (or more complicated topologies of couplings such as frustrating couplings) we abandoned the calculation on subsystems in the moment algorithm. In order not to be overwhelmed by the quickly rising dimension of the Hilbert space we identified the original trace with an expectation value on an extended Hilbert space. This trick reduces the number of terms in the application of the Hamiltonian from $L2^N$ to L where L is the number of bonds and N the number of sites. In the moment algorithm the inclusion of frustration is not more complicated than the inclusion of any other additional coupling. This is in contrast to quantum Monte Carlo approaches where frustration leads generically to the severe sign problem.

For not too low temperatures a very good agreement could be achieved. Including further information on the low temperature the agreement can be improved further. In particular, the use of information on the zero temperature dispersion turned out to be very efficient. In this way, even relatively low orders allow a good description of the thermodynamic quantities under study. The necessary dispersion information can be taken from exact or approximate results. Taking experimental dispersion results allows to check the consistency of the model assumed.

Due to the possibility to reach satisfactory results already in low orders of the high temperature expansion the application to higher dimensional cases such as the strongly frustrated Shastry-Sutherland model [40, 41] is possible and will be reported elsewhere. Work on gapped systems such as dimerised chains is in progress.

We acknowledge many useful discussions with E. Müller-Hartmann and H. Monien. We are indebted to A. Klümper for the Bethe ansatz data and to R. Raupach and F. Schönfeld for the DMRG results which we used as benchmarks. Equally, helpful remarks by A. Honecker are acknowledged. This work was supported by the Deutsche Forschungsgemeinschaft in the SFB 341 and in the Schwerpunkt 1073. The computations were mainly done on machines of the Regional Computing Center of the University of Cologne.

Appendix A: Coefficients

A.1 Unfrustrated chain, moment algorithm

Here the results for the unfrustrated chain are presented. The susceptibility and the specific heat have been computed up to order 16.

A.1.1 Susceptibility

n	a_n	n	a_n
0	$\frac{1}{4}$	9	$\frac{3\,737}{74\,317\,824}$
1	$-\frac{1}{8}$	10	$-\frac{339\,691}{5\,945\,425\,920}$
2	0	11	$-\frac{1\,428\,209}{54\,499\,737\,600}$
3	$\frac{1}{96}$	12	$\frac{18\,710\,029}{2\,242\,274\,918\,400}$
4	$\frac{5}{1\,536}$	13	$\frac{7\,045\,849}{809\,710\,387\,200}$
5	$-\frac{7}{5\,120}$	14	$-\frac{358\,847}{3\,957\,275\,492\,352}$
6	$-\frac{133}{122880}$	15	$-\frac{65\,174\,099\,663}{28\,566\,582\,460\,416\,000}$
7	$\frac{1}{16\,128}$	16	$-\frac{258\,645\,079\,463}{498\,616\,712\,036\,352\,000}$
8	$\frac{1\,269}{4\,587\,520}$		

Series coefficients a_n for the high temperature expansion of the magnetic susceptibility $\chi = \frac{1}{T}\sum_n a_n(\beta J)^n$.

A.1.2 Specific heat

n	a_n	n	a_n
0	0	9	$-\frac{4\,303}{688\,128}$
1	0	10	$-\frac{334\,433}{110\,100\,480}$
2	$\frac{3}{16}$	11	$\frac{37\,543}{31\,457\,280}$
3	$\frac{3}{32}$	12	$\frac{3\,987\,607}{3\,170\,893\,824}$
4	$-\frac{15}{256}$	13	$-\frac{1\,925\,339}{41\,523\,609\,600}$
5	$-\frac{15}{256}$	14	$-\frac{369\,233\,453}{930\,128\,855\,040}$
6	$\frac{21}{4\,096}$	15	$-\frac{31\,504\,270\,817}{362\,750\,253\,465\,600}$
7	$\frac{917}{40\,960}$	16	$\frac{851\,758\,334\,701}{8\,706\,006\,083\,174\,400}$
8	$\frac{1\,417}{327\,680}$		

Series coefficients a_n for the high temperature expansion of the magnetic specific heat $C = \sum_n a_n(\beta J)^n$.

A.2 Frustrated chain, moment algorithm

The coefficients for the results of frustrated chain are presented. The magnetic susceptibility and the magnetic specific heat are expanded up to order 10 in βJ.

A.2.1 Susceptibility

(n,k)	$a_{n,k}$	(n,k)	$a_{n,k}$	(n,k)	$a_{n,k}$	(n,k)	$a_{n,k}$	(n,k)	$a_{n,k}$	(n,k)	$a_{n,k}$
(0,0)	$\frac{1}{4}$	(4,1)	$-\frac{23}{768}$	(6,1)	$\frac{9}{1\,280}$	(7,5)	$\frac{943}{368\,640}$	(8,8)	$\frac{1\,269}{4\,587\,520}$	(10,0)	$-\frac{339\,691}{5\,945\,425\,920}$
(1,0)	$-\frac{1}{8}$	(4,2)	$\frac{1}{512}$	(6,2)	$\frac{221}{61\,440}$	(7,6)	$\frac{67}{368\,640}$	(9,0)	$\frac{3\,737}{74\,317\,824}$	(10,1)	$-\frac{22\,843}{1\,486\,356\,480}$
(1,1)	$-\frac{1}{8}$	(4,3)	$-\frac{1}{96}$	(6,3)	$-\frac{163}{92\,160}$	(7,7)	$\frac{1}{16\,128}$	(9,1)	$-\frac{34\,337}{23\,592\,960}$	(10,2)	$\frac{15\,205\,963}{5\,945\,425\,920}$
(2,0)	0	(4,4)	$\frac{5}{1\,536}$	(6,4)	$\frac{7}{15\,360}$	(8,0)	$\frac{1\,269}{4\,587\,520}$	(9,2)	$\frac{14\,125}{4\,128\,768}$	(10,3)	$-\frac{311\,903}{82\,575\,360}$
(2,1)	$\frac{1}{8}$	(5,0)	$-\frac{7}{5\,120}$	(6,5)	$\frac{23}{7\,680}$	(8,1)	$-\frac{23\,629}{20\,643\,840}$	(9,3)	$-\frac{1\,249}{35\,389\,440}$	(10,4)	$\frac{9\,659}{3\,932\,160}$
(2,2)	0	(5,1)	$-\frac{49}{6\,144}$	(6,6)	$-\frac{133}{122\,880}$	(8,2)	$-\frac{58\,651}{13\,762\,560}$	(9,4)	$\frac{317}{229\,376}$	(10,5)	$-\frac{1\,177\,787}{825\,753\,600}$
(3,0)	$\frac{1}{96}$	(5,2)	$\frac{37}{1\,536}$	(7,0)	$\frac{1}{16\,128}$	(8,3)	$\frac{28\,751}{5\,160\,960}$	(9,5)	$-\frac{969}{655\,360}$	(10,6)	$\frac{599\,639}{594\,542\,592}$
(3,1)	$\frac{1}{128}$	(5,3)	$-\frac{1}{128}$	(7,1)	$\frac{5\,863}{1\,474\,560}$	(8,4)	$-\frac{59}{20\,160}$	(9,6)	$\frac{93\,463}{61\,931\,520}$	(10,7)	$\frac{791\,221}{1\,486\,356\,480}$
(3,2)	$-\frac{1}{32}$	(5,4)	$\frac{1}{512}$	(7,2)	$-\frac{805}{73\,728}$	(8,5)	$-\frac{877}{1\,290\,240}$	(9,7)	$-\frac{67\,097}{82\,575\,360}$	(10,8)	$-\frac{367\,481}{1\,486\,356\,480}$
(3,3)	$\frac{1}{96}$	(5,5)	$-\frac{7}{5\,120}$	(7,3)	$\frac{3\,023}{737\,280}$	(8,6)	$\frac{5\,389}{20\,643\,840}$	(9,8)	$-\frac{361}{1\,720\,320}$	(10,9)	$\frac{22\,433}{148\,635\,648}$
(4,0)	$\frac{5}{1\,536}$	(6,0)	$-\frac{133}{122\,880}$	(7,4)	$-\frac{381}{81\,920}$	(8,7)	$-\frac{1\,271}{1\,720\,320}$	(9,9)	$\frac{3\,737}{74\,317\,824}$	(10,10)	$-\frac{339\,691}{5\,945\,425\,920}$

Series coefficients $a_{n,k}$ for the high temperature expansion of the magnetic susceptibility of the frustrated chain $\chi = \frac{1}{T}\sum_{n,k} a_{n,k}\alpha^k(\beta J)^n$.

A.2.2 Specific heat

(n,k)	$a_{n,k}$	(n,k)	$a_{n,k}$	(n,k)	$a_{n,k}$	(n,k)	$a_{n,k}$	(n,k)	$a_{n,k}$	(n,k)	$a_{n,k}$
(0,0)	0	(4,1)	$-\frac{3}{32}$	(6,1)	$\frac{63}{512}$	(7,5)	$-\frac{245}{8\,192}$	(8,8)	$\frac{1\,417}{327\,680}$	(10,0)	$-\frac{334\,433}{110\,100\,480}$
(1,0)	0	(4,2)	$-\frac{3}{32}$	(6,2)	$-\frac{363}{4\,096}$	(7,6)	0	(9,0)	$-\frac{4303}{688\,128}$	(10,1)	$\frac{92629}{2\,752\,512}$
(1,1)	0	(4,3)	0	(6,3)	$\frac{17}{512}$	(7,7)	$\frac{917}{40\,960}$	(9,1)	$\frac{2\,613}{573\,440}$	(10,2)	$-\frac{420475}{11\,010\,048}$
(2,0)	$\frac{3}{16}$	(4,4)	$-\frac{15}{256}$	(6,4)	$\frac{105}{1\,024}$	(8,0)	$\frac{1417}{327\,680}$	(9,2)	$\frac{3\,855}{57\,344}$	(10,3)	$\frac{59\,305}{2\,752\,512}$
(2,1)	0	(5,0)	$-\frac{15}{256}$	(6,5)	0	(8,1)	$-\frac{4\,793}{61\,440}$	(9,3)	$\frac{1}{10\,240}$	(10,4)	$-\frac{138\,811}{2\,752\,512}$
(2,2)	$\frac{3}{16}$	(5,1)	$\frac{25}{128}$	(6,6)	$\frac{21}{4\,096}$	(8,2)	$\frac{2\,323}{24\,576}$	(9,4)	$-\frac{261}{286\,720}$	(10,5)	$\frac{51\,701}{1\,376\,256}$
(3,0)	$\frac{3}{32}$	(5,2)	$-\frac{5}{128}$	(7,0)	$\frac{917}{40\,960}$	(8,3)	$-\frac{59}{960}$	(9,5)	$\frac{5\,901}{81\,920}$	(10,6)	$\frac{27\,641}{2\,752\,512}$
(3,1)	$-\frac{9}{32}$	(5,3)	$\frac{15}{128}$	(7,1)	$-\frac{2\,611}{40\,960}$	(8,4)	$\frac{35}{2\,048}$	(9,6)	$-\frac{2\,411}{143\,360}$	(10,7)	$-\frac{1\,817}{917\,504}$
(3,2)	0	(5,4)	0	(7,2)	$-\frac{119}{4\,096}$	(8,5)	$-\frac{407}{61\,440}$	(9,7)	$-\frac{2\,229}{573\,440}$	(10,8)	$\frac{38993}{1\,572\,864}$
(3,3)	$\frac{3}{32}$	(5,5)	$-\frac{15}{256}$	(7,3)	$-\frac{413}{4\,096}$	(8,6)	$-\frac{2\,449}{40\,960}$	(9,8)	0	(10,9)	0
(4,0)	$-\frac{15}{256}$	(6,0)	$\frac{21}{4\,096}$	(7,4)	$\frac{651}{20\,480}$	(8,7)	0	(9,9)	$-\frac{4\,303}{688\,128}$	(10,10)	$-\frac{334\,433}{110\,100\,480}$

Series coefficients $a_{n,k}$ for the high temperature expansion of the magnetic specific heat of the frustrated chain $C = \sum_{n,k} a_{n,k}\alpha^k(\beta J)^n$.

A.3 Unfrustrated chain, linked cluster expansion

A.3.1 Susceptibility

n	a_n	n	a_n	n	a_n	n	a_n	n	a_n
0	1.0	5	−4 032.0	10	−9 565 698 560.0	15	−205 019 990 184 689 664.0	20	−18 366 266 410 738 921 187 573 760.0
1	-4.0	6	−89 376.0	11	−210 597 986 304.0	16	−3 169 755 454 477 500 416.0	21	−40 780 317 289 246 872 850 923 520.0
2	0.0	7	163 840.0	12	3 486 950 684 672.0	17	208 763 541 109 969 256 448.0	22	38 668 138 493 195 891 009 425 244 160.0
3	64.0	8	26 313 984.0	13	203 634 731 188 224.0	18	8 342 101 010 835 559 022 592.0	23	983 734 184 997 038 611 238 624 428 032.0
4	400.0	9	191 334 400.0	14	-127 324 657 152 000.0	19	−175 912 858 271 144 581 529 600.0	24	−75 650 797 544 886 562 610 211 717 119 286.7

Series coefficients for the linked cluster expansion of the magnetic susceptibility for the Heisenberg chain with $\chi = \frac{1}{4T}\sum_n \frac{a_n}{(n+1)!}(\frac{J}{4T})^n$.

A.3.2 Specific heat

n	a_n	n	a_n	n	a_n	n	a_n	n	a_n
0	0.0	5	−7 200.0	10	-11 558 004 480.0	15	−121 944 211 136 778 240.0	20	96 147 483 542 540 314 214 400.0
1	0.0	6	15 120.0	11	199 812 856 320.0	16	8 791 781 390 116 945 920.0	21	1 279 121 513 829 538 179 364 945 920.0
2	6.0	7	1 848 672.0	12	10 106 191 180 800.0	17	310 402 124 957 945 954 304.0	22	27 962 069 861 743 501 862 336 200 704.0
3	36.0	8	11 426 688.0	13	-19 376 365 252 608.0	18	−7 225 535 925 744 106 143 744.0	23	−2 398 518 627 113 966 015 427 501 883 392.0
4	−360.0	9	−594 846 720.0	14	-9 289 795 522 775 040.0	19	-643 407 197 363 813 620 776 960.0	24	−129 834 725 539 335 848 980 192 847 460 554.1120

Series coefficients for the linked cluster expansion of the magnetic specific heat for the Heisenberg chain with $C = \sum_n \frac{a_n}{n!}(\frac{J}{4T})^n$.

References

1. D.C. Johnston *et al.*, `cond-mat/0001147 (2000)`.
2. K. Fabricius, U. Löw, J. Stolze, Phys. Rev. B **55**, 5833 (1997).
3. R. Bursill *et al.*, J. Phys. Cond. Matter **7**, 8605 (1995).
4. N. Shibata, J. Phys. Soc. Jpn **66**, 2221 (1997).
5. X.Q. Wang, T. Xiang, Phys. Rev. B **56**, 5061 (1998).
6. D.C. Johnston *et al.*, Phys. Rev. B **61**, 9558 (2000).
7. H.-X. He, C.J. Hamer, J. Oitmaa, J. Phys. A **23**, 1775 (1990).
8. M.P. Gelfand, R.R.P. Singh, D.A. Huse, J. Stat. Phys. **59**, 1093 (1990).
9. G.A. Baker, G.S. Rushbrooke, H.E. Gilbert, Phys. Rev. **135**, A1272 (1964).
10. T. Obokata, I. Ono, T. Oguchi, J. Phys. Soc. Jpn **23**, 516 (1967).
11. A. Klümper, Z. Phys. B **91**, 507 (1993).
12. A. Klümper, Eur. Phys. J. B **5**, 677 (1998).
13. A. Klümper, R. Raupach, F. Schönfeld, Phys. Rev. B **59**, 3612 (1999).
14. G. Müller, H. Thomas, H. Beck, J.C. Bonner, Phys. Rev. B **24**, 1429 (1981).
15. J. des Cloizeaux, J.J. Pearson, Phys. Rev. **128**, 2131 (1962).
16. A. Fledderjohann, C. Gros, Europhys. Lett. **37**, 189 (1997).
17. S. Eggert, Phys. Rev. B **54**, R9612 (1996).
18. B.S. Shastry, B. Sutherland, Phys. Rev. Lett. **47**, 964 (1981).
19. I. Affleck, in *Dynamical Properties of Unconventional Magnetic Systems*, edited by A.T. Skjeltorp, D. Sherrington (Kluwer Academic Publishers, 1997).
20. G.S. Uhrig, F. Schönfeld, M. Laukamp, E. Dagotto, Eur. Phys. J. B **7**, 67 (1999).
21. M. Hase, I. Terasaki, K. Uchinokura, Phys. Rev. Lett. **70**, 3651 (1993).
22. J.P. Boucher, L.P. Regnault, J. Phys. I France **6**, 1939 (1996).
23. J. Riera, A. Dobry, Phys. Rev. B **51**, 16098 (1995).
24. G. Castilla, S. Chakravarty, V.J. Emery, Phys. Rev. Lett. **75**, 1823 (1995).
25. K. Fabricius *et al.*, Phys. Rev. B **57**, 1102 (1998).
26. C. Knetter, G. S. Uhrig, in preparation.
27. To be cautious, we re-state that statements on the validity of $1/T$ results depend on the representation used.
28. G.S. Uhrig, H.J. Schulz, Phys. Rev. B **54**, R9624 (1996); *Err.* **58**, 2900 (1998).
29. M. Troyer, H. Tsunetsugu, D. Würtz, Phys. Rev. B **50**, 13515 (1994).
30. G.S. Uhrig, B. Normand, Phys. Rev. B **58**, R14705 (1998).
31. B. Lüthi, private communication (2000).
32. H. Kageyama *et al.*, accepted in Phys. Rev. Lett., `cond-mat/0005342`.
33. L.D. Faddeev, L.A. Takhtajan, Phys. Lett. **85A**, 375 (1981).
34. M. Karbach *et al.*, Phys. Rev. B **55**, 12510 (1997).
35. M. Abramowitz, I.A. Stegun, *Handbook of Mathematical Functions* (Dover Publisher, New York, 1964).
36. R.B. Griffiths, Phys. Rev. **133**, A768 (1964).
37. C.N. Yang, C.P. Yang, Phys. Rev. **151**, 258 (1966).
38. S. Lukyanov, Nucl. Phys. B **522**, 533 (1998).
39. C. Knetter, G.S. Uhrig, Eur. Phys. J. B **13**, 209 (2000).
40. H. Kageyama *et al.*, Phys. Rev. Lett. **82**, 3168 (1999).
41. Z. Weihong, C.J. Hamer, J. Oitmaa, Phys. Rev. B **60**, 6608 (1999).